

THE PHYSICAL REVIEW

A journal of experimental and theoretical physics established by E. L. Nichols in 1893

SECOND SERIES, VOL. 81, No. 6

MARCH 15, 1951

The Altitude and Latitude Variation in the Rate of Occurrence of Nuclear Disintegrations Produced in the Stratosphere by Cosmic Rays*

J. J. LORD

Department of Physics, University of Chicago, Chicago, Illinois

(Received October 19, 1950)

The variation with altitude of the rate of production of stars in photographic plates was measured from mountain elevations to 94,000 feet at geomagnetic latitude $\lambda \approx 54^\circ \text{N}$. The type of particle initiating each star was determined and showed that the total flux of star-producing protons decreased rapidly from 94,000 feet to 11,500 feet and was compatible with an absorption mean free path (m.f.p.) of 145 g/cm². The total flux of star-producing neutrons showed a maximum near 70,000 feet and then decreased with altitude with an absorption mean free path of 170 g/cm². Similar altitude dependence measurements were made at $\lambda \approx 28^\circ \text{N}$ and showed that the rate of production by neutrons of stars of 3

to 9 prongs at 94,000 feet was 0.19 of the corresponding value at $\lambda \approx 54^\circ$. This demonstrates that 81 percent of the small stars at $\lambda \approx 54^\circ$ must be due to the primary particles of the cosmic radiation in the energy intervals given by the geomagnetic cut-off at $\lambda \approx 28^\circ$ and $\lambda \approx 54^\circ$ (1 to 8 Bev for protons, and for α -particles and heavy nuclei 0.35 to 3.5 Bev per nucleon). The total flux of star-producing protons varies by a factor of 3.0 between these two latitudes at 94,000 feet and shows that 67 percent of the proton-initiated stars at $\lambda \approx 54^\circ$ are due to primary particles of the energies given above.

I. INTRODUCTION

A CONSIDERABLE insight into the nature and interactions of high energy cosmic-ray particles can be obtained from the variation with altitude and latitude of the rate of production of nuclear disintegrations. A large number of investigations have been conducted in the lower atmosphere from sea level to mountain elevations by means of photographic emulsion techniques.¹ In addition, some experiments were also performed in airplanes up to altitudes of about 35,000 feet at northern latitudes.²

In the stratosphere, at northern latitudes, preliminary measurements of the total nuclear disintegration intensity, using plates of low sensitivity, have been made at four different altitudes.³ Many other measurements,^{4,5} mostly with low sensitivity plates, have been

made at only single altitudes. However, in some of these cases the general trend in the altitude variation of nuclear disintegrations in the stratosphere could be deduced.^{3,5} The rate of production of nuclear disintegrations in photographic emulsions has been measured at a number of different latitudes from sea level to mountain elevations.⁶ In the stratosphere measurements have been carried out at only two different latitudes.⁷

The majority of the above investigations have been conducted with photographic plates of low sensitivity which record only particles of moderate energies. In the investigations reported in the following paper, photographic plates sensitive to charged particles of all energies were used to measure the latitude and altitude dependence of the rate of production of stars. The altitude variation in the stratosphere of stars produced by neutrons, protons, alpha-particles, and heavy nuclei yields information as to the type of interactions pro-

* Assisted by the joint program of the ONR and AEC.

¹ Lattes, Occhialini, and Powell, *Nature* **160**, 453 (1947); D. H. Perkins, *Nature* **160**, 707 (1947); Bernardini, Cortini, and Manfredini, *Nuovo cimento* **5**, 511 (1948); G. E. Belovitskii, and L. V. Sukhov, *Doklady Akad., Nauk SSSR* **62**, No. 2, 207 (1948); E. P. George, and A. C. Jason, *Proc. Phys. Soc. (London)* **A62**, 243 (1949); Brown, Camerini, Fowler, Heitler, King, and Powell, *Phil. Mag.* **40**, 862 (1949).

² Nora Page, *Proc. Phys. Soc. (London)* **A63**, 250 (1950); H. H. Foster, *Phys. Rev.* **78**, 247 (1950).

³ M. Schein and J. J. Lord, *Phys. Rev.* **73**, 189 (1948); J. J. Lord and M. Schein, *Phys. Rev.* **75**, 1957 (1949).

⁴ Salant, Hornbostel, and Dollmann, *Phys. Rev.* **74**, 694 (1948); M. Addario and S. Tamburino, *Phys. Rev.* **76**, 983 (1949);

Yagoda, Kaplan, and Conner, *Phys. Rev.* **76**, 171 (1949); Camerini, Coor, Davies, Fowler, Lock, Muirhead, and Tobin, *Phil. Mag.* **40**, 1073 (1949).

⁵ Freier, Ney, and Oppenheimer, *Phys. Rev.* **75**, 1451 (1949).

⁶ Beets, Morand, and Winand, *Compt. rend.* **229**, 1227 (1949); H. Yagoda, *Echo Lake Cosmic-Ray Symposium* (1949), unpublished.

⁷ E. O. Salant, *Echo Lake Cosmic-Ray Symposium* (1949), unpublished.

duced by the primary cosmic-ray particles. Further, the stars produced by neutrons show both the manner in which primary particles produce secondary nucleons in the atmosphere and the manner in which these secondary particles lose their energy. The variation with latitude of these phenomena then shows the dependence of the nuclear disintegrations and the production of secondary particles on the energy of the primary particles.

II. EXPERIMENTAL PROCEDURES

(A) Apparatus

All investigations described in this paper were carried out with Ilford G-5 emulsions in order to avoid, as much as possible, any difference in measurement which may occur in using emulsions of various types. For each measurement a sandwich of 6 to 12 plates, two inches by two inches, were employed with the emulsions of adjacent plates in direct contact. Each group of plates was then covered with a single layer of Cellophane, and

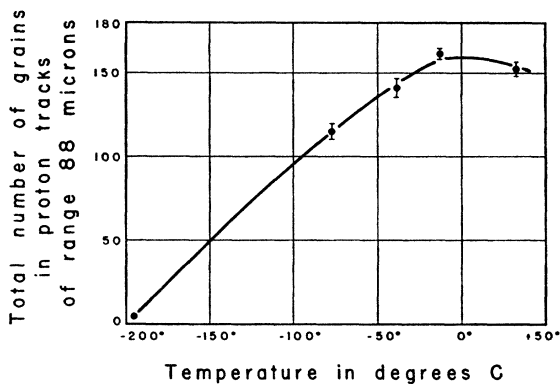


FIG. 1. Temperature sensitivity of photographic emulsions.

then about four layers of 0.002-inch thick aluminum foil to protect the emulsions from visible radiation. The plates were always located with the surfaces of the emulsions parallel to the zenith direction.

Near-by matter in sufficient quantities can effect the rate of star production by a factor as large as 50 percent. For this reason each group of plates was placed in a small cubical celluloid-covered Dow metal balloon gondola of the dimension of 10 inches on each edge. The total mass of the gondola and the plates was close to 300 grams. About 50 percent of the area of the balloon gondola was covered with aluminum foil in order to eliminate the excessive heating effect of the sunlight. With the arrangement just mentioned the temperature of the plates was kept between -5° and $+10^{\circ}\text{C}$ on each individual flight. The sensitivity of the plates is not appreciably affected by temperature under the above conditions of exposure. This can be seen from the graph in Fig. 1, showing the variation of grain density with temperature of 3-Mev proton tracks. These results are

⁸ J. J. Lord and M. Schein, *Phys. Rev.* **75**, 1956 (1949).

in essential agreement with the measurements of Dilworth and Dollmann.⁹ Measurements of the grain density of minimum ionization tracks show that the grain density decreases by less than 10 percent for a decrease of temperature from $+20^{\circ}$ to approximately -50°C , which is considerably less than for heavily ionizing tracks as shown in Fig. 1.

(B) Method of Exposure in the Stratosphere

The small balloon gondolas described above were attached to the rigging from either a cluster of K2000-type balloons or a single large plastic balloon.¹⁰ In each case the gondola with plates was located at least 15 feet above any material being used for other experiments on the same balloon flight. The constancy of the measured intensity of stars at 1.1-cm Hg pressure-altitude for a number of separate flights demonstrated that the above arrangement of plates was free of any influence of material when kept at least 15 feet below the plates.

The pressure-altitude for the cluster balloon flights was determined with both a recording aneroid type barometer and, for greater accuracy at less than 15-cm Hg pressure, a recording Hg U-tube pressure gage. In the aneroid barometer, expansion of the bellows moved a small lever arm at the end of which was attached a pen. The pen produced a line on a clock-driven paper disk, and the amplitude of this line was proportional to the pressure. The most serious source of error in pressure readings, measured with aneroid type barometers, is due to variations of temperature. To avoid this difficulty only standard radiosonde bellows and lever arms made up with bimetal elements were employed. Those barometers which were selected for use showed less than three millimeters change in pressure for a temperature change of at least 20°C .

The Hg U-tube barometer utilized a beam of light, falling on one arm of a U-tube placed before a slit. Behind the slit a clock-driven drum, covered with a piece of photographic paper, revolved slowly. As pressure changes altered the level of the mercury in the

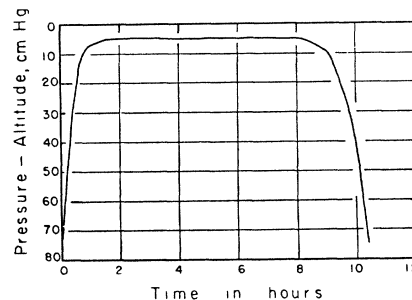


FIG. 2. A typical free balloon flight time *versus* pressure-altitude curve.

⁹ C. C. Dilworth, *Cosmic Radiation* (Interscience Publishers, Inc., New York, 1949), p. 157. E. M. Dollmann, *Rev. Sci. Instr.* **21**, 118 (1950).

¹⁰ These balloon flights were made possible through the courtesy of the ONR and the General Mills Company.

tube, the length of the section of the slit under illumination was changed by a corresponding amount. The Hg U-tube barometer, owing to the short column of Hg (about 10 cm), is not affected appreciably by temperature changes occurring on any of the balloon flights. The pressure readings obtained from this barometer are accurate to 0.5 mm.

The pressure-altitude vs time curve for a typical flight at low altitude is given in Fig. 2. In this flight a cluster of 12 balloons was used, which reached their ceiling pressure-altitude of 4.7 cm Hg 1.5 hours after release. After a number of balloons had burst, the equipment remained almost at a fixed pressure-altitude for 8.6 hours. Then a few more balloons burst and the equipment descended slowly to earth with 4 balloons still inflated. The essential data regarding the other flights used in this investigation are given in Table I.

(C) Determination of the Volume of Emulsions

The plates employed in these measurements were all developed by the temperature variation method. In

TABLE I. Balloon flights.

Date of flight	Average ceiling pressure-altitude in cm of Hg	Time in hours at ceiling pressure-altitude	Geo-magnetic latitude
April 2, 1949	1.0	5.8	55°N
May 26, 1949	1.0	4.1	55°N
July 22, 1949	1.0	6.8	55°N
September 15, 1949	1.1	7.1	55°N
August 3, 1949	3.5	6.5	55°N
March 30, 1950	4.7	8.6	53°N
August 30, 1949	6.0	1.8	55°N
May 29, 1949	8.0	2.8	53°N
November 15, 1949	1.1	6.6	28°N
November 14, 1949	3.5	8.4	28°N

order to determine the rate of production of nuclear disintegrations in the photographic emulsions, it was necessary to know, prior to processing the volume, the composition and density of the portions of each emulsion examined. The composition of the emulsion is given by Ilford in a small information circular attached to each box of plates. The composition and related relevant data are given in Table II. The plates delivered had a very uniform composition; however, the figures given for the composition in Table II are at best only approximate. For this reason it was found that the most accurate method for finding the frequency of nuclear events in the emulsion would be in terms of the rate per gram of emulsion. As can be seen in Table II, the heavy elements, silver and bromine, account for about 70 percent of the total geometrical cross section for nuclear events occurring in the emulsion. The measurements of Perkins and Harding¹¹ show that this is actually the case.

¹¹ J. B. Harding, Nature 163, 440 (1949).

TABLE II. Compositions and cross sections of Ilford G-5 emulsion.

Element	Atomic weight A_i	Density of emulsion components in g/cc ρ_i	Number of atoms per cc N_i	cross section per nucleus in cm ² σ_i	Cross section of N_i nuclei per cc $N_i \times \sigma_i$
¹⁰⁷ Ag	107.9	1.85	1.056×10^{22}	1.338×10^{-24}	1.411×10^{-2}
¹³⁵ Br	79.9	1.36	1.025×10^{22}	1.094×10^{-24}	1.121×10^{-2}
¹²⁷ I	126.9	0.024	0.01139×10^{22}	1.49×10^{-24}	1.698×10^{-4}
¹² C	12.0	0.27	1.3545×10^{22}	0.309×10^{-24}	4.18×10^{-3}
¹ H	1.01	0.056	3.34×10^{22}	0.0594×10^{-24}	19.8×10^{-4}
¹⁶ O	16.0	0.27	0.939×10^{22}	0.3745×10^{-24}	3.52×10^{-3}
³² S	32.1	0.010	0.01873×10^{22}	0.596×10^{-24}	11.18×10^{-6}
¹⁴ N	14.0	0.067	0.2875×10^{22}	0.343×10^{-24}	9.86×10^{-4}
Total		3.907	8.032×10^{22}		361.67×10^{-4}

The total nuclear cross section per gram of emulsion is given in terms of the symbols in Table II by the following equation:

$$\sigma_T / \rho_T = [N_0 \sum_i (\rho_i / A_i) \sigma_i] / (\sum_i \rho_i), \quad (1)$$

where N_0 =Avogadro's number, A_i =atomic weight of component i of emulsion, ρ_i =density of component i of emulsion, σ_i =geometrical cross section of nucleus of component i , σ_T =cross section per cc of emulsion, ρ_T =density of emulsion. From the approximate values of the composition given in Table II in the above formula it follows directly that a given percentage change in the composition of silver or bromine results in a change of one-fourth of this amount in the cross section per gram. Thus, the frequency of nuclear collisions per gram will be quite insensitive even to quite appreciable changes in the composition of the emulsion.

While the plates for each balloon flight were being chosen, several sample plates were selected at random and set aside for the purpose of determining the mass of the emulsion per square centimeter. The sample plates selected were carefully divided into two sections, and one-half of each was processed in the same manner as those used for the balloon flight. Measurements of mass, thickness,¹² and area of emulsion were then made

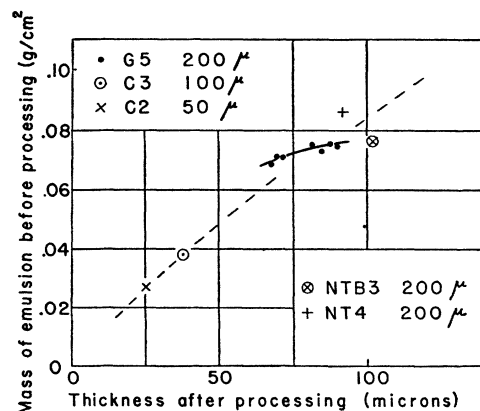


FIG. 3. The mass per square centimeter of emulsions before processing in terms of the thickness after processing.

¹² The emulsion and glass backing of the plate were weighed together first; and then, after the emulsion had been removed completely with acid, the weight of the glass backing alone was subtracted from the total to give the weight of the emulsion.

on both the processed and the unprocessed portions. The relation, as obtained from the sample plates, between the mass per square centimeter of the emulsion, before processing, to the thickness after processing is given in Fig. 3 and compared with several other types and thicknesses of plates. It can be seen, Fig. 3, that for the 200-micron thick plates, used in this investigation, the thickness, after processing, provides a very accurate measure of the original mass per square centimeter. The average thickness of each emulsion examined was measured with an accuracy of 2 percent, and from the curve in Fig. 3 it follows directly that the mass of the emulsion before processing is then known to an accuracy of 1 percent. The area of each emulsion examined was measured to 0.5 percent with a standard microscope stage.

The intensities of stars determined per gram of emulsion were multiplied by 3.91, the average density of the emulsion, so that the measurements could be compared directly with those data of other investigations in which the intensities are given per cubic centimeter.

(D) Scanning and Examination of Plates

All of the emulsions used were scanned carefully with a binocular microscope employing a total magnification of 210. This power is higher than is needed for the detection of most events, but is quite necessary for good efficiency¹³ in locating small stars and mesons. The detection efficiency of large stars was always greater than 99 percent, but many of the plates had to be scanned several times in order for an efficiency greater than 97 percent to be obtained for the detection of all stars.

After the events had been located in the scanning operation, each was re-examined using a 90-power oil immersion objective, thus obtaining the exact number of tracks per star. All tracks from stars having a grain density corresponding to an energy loss less than seven times the minimum value were examined in detail. The spatial angles and grain densities of each of these tracks was determined. The angle formed by the projection of the track in the plane of the emulsion surface was measured with a goniometer ocular. The tangent of the angle between the track and the plane of the emulsion surface was determined from the ratio of the horizontal projected length of the track and the vertical distance, corrected for emulsion shrinkage, measured with a specially calibrated microscope fine adjustment movement.

III. THE RATE OF PRODUCTION OF COSMIC-RAY STARS IN THE STRATOSPHERE

(A) Determination of the Frequency of Stars

This investigation contains the determination of the rate of production of stars at a number of specific alti-

tudes in the stratosphere. As can be seen from the pressure *versus* time curves for typical flights³ (Fig. 2), corrections have to be made for those stars which occurred during the period of ascent and descent of the balloon. In addition, the photographic plates were exposed at sea level for a few days; and, since they were transported by air from London to Chicago, some of the cosmic-ray stars were produced during this time. All of the above factors were carefully taken into consideration; and it was found that, depending upon the altitude and length of the balloon flight, the corrections were between 2 and 7 percent of the total number of stars. The number of stars per gram of emulsion which were produced prior to the balloon flight was determined from several sample plates developed just before the flight. The corrections for the time of ascent and descent were obtained in two different ways. (a) For the balloon flights at geomagnetic latitudes of $\lambda = 27^\circ\text{N}$ to $\lambda = 29^\circ\text{N}$, several plates placed in a separate gondola were released on the ascent at a pressure-altitude of 3.5 cm Hg (70,000 feet). This made it possible to subtract from the total all stars which were produced below this altitude. (b) At geomagnetic latitudes $\lambda = 52^\circ\text{N}$ to $\lambda = 56^\circ\text{N}$ the corrections during the time of ascent and descent were made by carrying out a numerical integration of the following expression:

$$N(x) = I_P(x) \int_0^T f_x(p-P) dt,$$

where $N(x)$ = total number of stars per cc having x prongs as measured in the emulsion, P = average pressure-altitude at which balloon flight leveled off, $I_P(x)$ = rate of production of stars with x prongs per cc per day at pressure-altitude P , $f_x(p-P)$ = variation with pressure-altitude of rate of production of stars having x prongs and normalized to unity at $p = P$, t = time in hours, and T = total length of flight in hours. The approximate value of $f_x(p-P)$ was taken from previous measurements³ and $I_P(x)$, the rate of production of stars with x prongs for each balloon flight leveling off at the

TABLE III. Rate of production of stars.

Type of star (number of prongs)	Rate of production of stars per cc per day							Geo-magnetic latitude $\lambda \approx 27^\circ\text{N} - 29^\circ\text{N}$	
	Geomagnetic latitude $\lambda = 52^\circ\text{N} - 56^\circ\text{N}$							Pressure-altitude in cm Hg	
	1.1	3.5	4.7	6.0	8.9	50.0	1.1	3.5	
greater than 2	2390	2030	2150	2040	1610	22.0	575	425	
3, 4, and 5	1030	1059	1162	1210	820	18.2	215	187	
6, 7, 8, and 9	742	619	616	520	422	2.6	127	106	
greater than 9	618	352	372	235	290	1.2	238	132	
greater than 16	223	122	128	27	116	0.29	105	61	

¹³ G. Cortini and A. Manfredini, Nature **163**, 991 (1949).

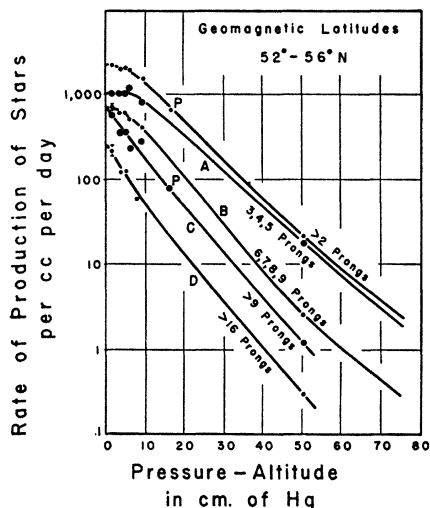


FIG. 4. Rate of production of stars as a function of pressure-altitude at $\lambda \approx 54^\circ\text{N}$.

pressure altitude P , was calculated. With these values of $I_P(x)$, more accurate values of $f_x(p-P)$ were calculated. This method of successive approximations was repeated until a value of $f_x(p-P)$ was found within the same limit of error as the actually measured values of $I_P(x)$.

(B) Altitude Variation ($\lambda = 52^\circ\text{--}56^\circ\text{N}$ and $\lambda = 27^\circ\text{--}29^\circ\text{N}$)

In Table III the results of the star intensity measurements at $\lambda = 52^\circ\text{--}56^\circ\text{N}$ are given as based on 8 balloon flights and plates exposed at Climax, Colorado (50 cm Hg pressure $\lambda = 48^\circ\text{N}$). The data in the table is plotted in Fig. 4, and the slope of the portions of the curves extending to sea level were obtained from the measurements of George and Jason.¹ The two points marked P in Fig. 4 were taken from the measurements of Page² and normalized to the intensities at Climax, Colorado. The altitude variation of stars according to prongs showed sufficient regularity that the stars were grouped as indicated on each curve in Fig. 4.

It can be seen from curve A, Fig. 4, that the rate of production of stars of 3, 4, and 5 prongs increases very nearly exponentially with atmospheric pressure from sea level to about 6 cm Hg. Near 6 cm Hg this rate of star production then quickly ceases to increase and remains almost constant up to the highest elevations reached in this investigation, 1.1 cm Hg (94,000 feet). Curve B, the rate of production of stars of 6, 7, 8, and 9 prongs is similar to curve A except that there is a slow increase in the rate of star production in the interval from 6.0 to 1.1 cm Hg. Both curves C and D differ markedly from A and B in that they show that the rate of production of larger stars of, respectively, more than 9 and more than 16 prongs increases rapidly with elevation from sea level to 1.1 cm Hg.

Considerable information as to the manner in which

star-producing particles are absorbed in air can be obtained if the simplifying but reasonable assumption is made that each particle causes a nuclear disintegration in which either (a) no further star-producing particles are emitted or (b) the emitted star-producing particles are produced in the same direction as the incident particle. The rate of production of stars in a thin photographic emulsion is proportional to the integrated flux of star-producing particles, J (number of particles per second passing through a sphere of 1 cm² cross-sectional area). If the intensity, I_0 , of incident particles per cm² per sec per steradian at the top of the atmosphere is taken to be independent of zenith angle, it can easily be shown that the integrated flux $J(y)$ at any depth in the atmosphere y is given by:

$$J(y) = \int_0^{90^\circ} I_0 \exp(-y/L_0 \cos\theta) \sin\theta d\theta, \quad (2)$$

where θ = zenith angle, y = depth in the atmosphere in g/cm², L_0 = absorption mean free path for nuclear collisions per cm².

The slope of the curves $J(y)$ vs y can be made equal to that of any portion of the rate of star production curves in Fig. 4 by adjustment of L_0 , the absorption mean free path for nuclear collisions. This gives a value of $L_0 = 165$ g/cm² for particles producing the stars of 3, 4, and 5 prongs at pressures greater than 15 cm Hg. The curve $J(y)$ can be made to fit quite well all of the measured values of the rate of production of stars of more than 16 prongs for $L_0 = 120$ g/cm². It is obvious from the curves in Fig. 4 that the absorption mean free path for particles producing small stars has no meaning in the region between 1.1- and 10-cm Hg pressure, since in this region star-producing secondary particles are being produced by the primaries very abundantly.

In Table III data are given for the rate of star production at two different balloon altitudes at $\lambda = 27^\circ\text{--}$

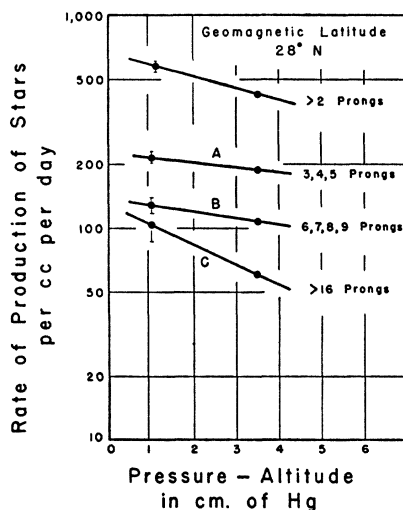


FIG. 5. Rate of production of stars as a function of pressure-altitude at $\lambda \approx 28^\circ\text{N}$.

TABLE IV. Variation in the rate of star production between $\lambda \approx 28^\circ$ and $\lambda \approx 54^\circ$.

Type of star (number of prongs)	Rate of production per cc per day		Ratio: rate at 54°N divided by rate at 28°N
	$\lambda \approx 54^\circ$	$\lambda \approx 28^\circ$	
> 3	1950 ± 100	530 ± 38	3.7 ± 0.3
3, 4, 5	1030 ± 100	215 ± 17	4.8 ± 0.6
6, 7, 8, 9	742 ± 50	127 ± 20	5.8 ± 0.9
> 9	618 ± 50	238 ± 15	2.6 ± 0.2
> 16	223 ± 25	105 ± 20	2.1 ± 0.4

29°N . These data are plotted in Fig. 5, where it can be seen from curve A that the rate of production of stars of 3, 4, and 5 prongs undergoes a slight decrease from 1.1- to 3.5-cm Hg pressure, while the stars of 6, 7, 8, and 9 prongs, curve B, show a somewhat larger decrease in the same interval. In contrast to this, the rate of production of the larger stars of more than 16 prongs, curve C, shows a very large decrease by a factor of 1.7 in the interval from 1.1 to 3.5 cm Hg. Applying expression (2) to curve C (Fig. 5) the rate of production of stars of more than 16 prongs gives a value of the absorption mean free path L_0 equal to 130 g/cm^2 , which is approximately the same as the corresponding value of 125 g/cm^2 at $\lambda \approx 54^\circ\text{N}$.

Although few data are available for the rate of star production at mountain elevations near $\lambda \approx 28^\circ\text{N}$, a good estimate of the total rate of star production at 43 cm Hg can be obtained from the general latitude variation measurements of Beets, Morand, and Winand,¹⁴ which are in general agreement with the nuclear disintegration measurements of Simpson and Uretz.¹⁴ From the former data,¹⁴ the rate of production of stars of more than 3 prongs was calculated to be 15.5 per cc per day at 43 cm Hg and at $\lambda \approx 28^\circ\text{N}$. The above rate at 43 cm Hg and the rate of 3.5 cm Hg from Table III can be used in expression (2) and gives an absorption mean free path of $L_0 = 220 \text{ g/cm}^2$, which is to be compared with the corresponding value of $L_0 = 165 \text{ g/cm}^2$ at $\lambda \approx 54^\circ\text{N}$.

The variation with latitude of stars as a function of the number of prongs is given in Table IV for the flights at 1.1 cm Hg ($\lambda \approx 54^\circ$ and $\lambda \approx 28^\circ$). The complete curves for star frequency *vs* prong numbers at two different latitudes are given in Fig. 6. The two curves in Fig. 6 show that the rate of production of stars of more than 25 prongs is almost independent of latitude, which definitely means that they are predominantly produced by particles with energies in excess of the minimum values allowed by the magnetic field of the earth at $\lambda \approx 28^\circ$ (8 Bev for protons and 3.5 Bev per nucleon for heavy nuclei in the vertical direction).¹⁵ The rate of production of stars of small prong number up to 9 changes between $\lambda \approx 28^\circ$ and $\lambda \approx 54^\circ$ by a factor as large as 5 (Table IV). However, these stars are largely pro-

duced by neutrons, as will be shown later, and hence do not give direct information regarding the latitude effect for primary particles. It is interesting to note in this connection that the latitude-sensitive stars produced by primaries must largely be those having roughly 10 to 25 prongs (see Fig. 6) which would then be produced by protons of energies limited by the earth's magnetic field of 1 to 8 Bev and heavier nuclei from 0.35 to 3.5 Bev per nucleon.

(C) The Flux of Particles Producing Stars

Each star produced in the emulsion was examined carefully in order to determine the type of particle producing it. If one of the star tracks corresponded to that due to a singly charged particle of ionization energy loss less than 1.4 times the minimum value, and was located in the upper hemisphere (zenith angle between 0° and 90°), this track was considered to be due to the incident particle. The zenith angle distribution of singly

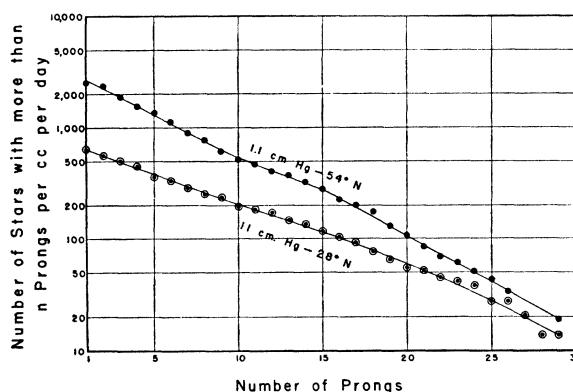


FIG. 6. Rate of production of stars with more than n prongs per cc per day at 94,000 feet as a function of the number of prongs n . The upper curve refers to $\lambda \approx 54^\circ$ and the lower $\lambda \approx 28^\circ$.

charged particles producing stars at 1.1 cm Hg, as will be discussed later (Fig. 7), shows that the tracks are sufficiently collimated about the vertical direction that an error of only a few percent would be made by the above method of selection of incident singly charged particles. π -mesons are known to decay in such a short time that their contribution to the production of stars in the rarified atmosphere at balloon elevations can be shown to be less than about 2 percent of the total stars. Thus, all singly charged particles producing stars will be considered to be protons.

Since tracks of minimum ionization of very short lengths are often difficult to find, only stars which were at least 15 microns from either surface of the processed emulsion were included in the measurements made to determine the types of particles producing stars. The average shrinkage factor for these emulsions was about 2.4, so that the minimum track length examined was about 35 microns; and owing to the collimation about the vertical direction of incident tracks, the average length was considerably longer. Measurements of the

¹⁴ Beets, Morand, and Winand, *Compt. rend.* **229**, 1227 (1949).
J. A. Simpson and R. B. Uretz, *Phys. Rev.* **76**, 569 (1949).

¹⁵ M. S. Vallarta, *Phys. Rev.* **74**, 1837 (1948).

decay electron tracks from μ -mesons showed that the detection efficiency was almost constant for angles ψ between the track and the surface of the emulsion, but fell off rapidly for angles ψ larger than 80° . Since positive μ -mesons from π - μ -disintegrations in the emulsion always decay with the emulsion of an electron, the absolute detection efficiency of these minimum ionization tracks was measured to be nearly 90 percent. For the majority of the incident protons close to minimum ionization which produce stars, the angle ψ is small (less than 50°), so that the detection efficiency for these protons must be greater than 95 percent.

Those stars in which a track was located in the upper hemisphere which corresponded to an ionization between 3 and 5 times the minimum value were examined to see if the star could have been produced by an alpha-particle because an alpha-particle with sufficient energy to produce a star would have an ionization in this range. That such a possibility exists was demonstrated by the fact that the distribution of ionization of all star tracks in the upper hemisphere which would be incident tracks showed a small peak at 4 times the minimum value. After subtraction of the background, the tracks located in this peak represented the number of alpha-particles which produced stars in the emulsion. The stars produced by nuclei heavier than boron were detected directly by the high delta-ray density on the incident track. The remaining stars in which no charged incident track could be identified were assumed to be produced by neutrons.

The rate of production of stars per cc per day by protons, neutrons, alpha-particles, and heavy nuclei is given in Table V at 1.1-cm Hg pressure for $\lambda \approx 54^\circ$ and $\lambda \approx 28^\circ$. The integrated flux of particles J_a per sec can be determined if the interaction mean free path is known for each type of particle producing stars. For an emulsion thin compared with the interaction mean free path, it can be shown that:

$$J_a = (L_a/3.91) \times (N_a/86,400), \quad (3)$$

where J_a = flux of particles of type a per sec passing through a sphere of 1-cm² cross-sectional area, L_a = the collision mean free path in g/cm² for an emulsion of average density 3.91, N_a = the rate of production of

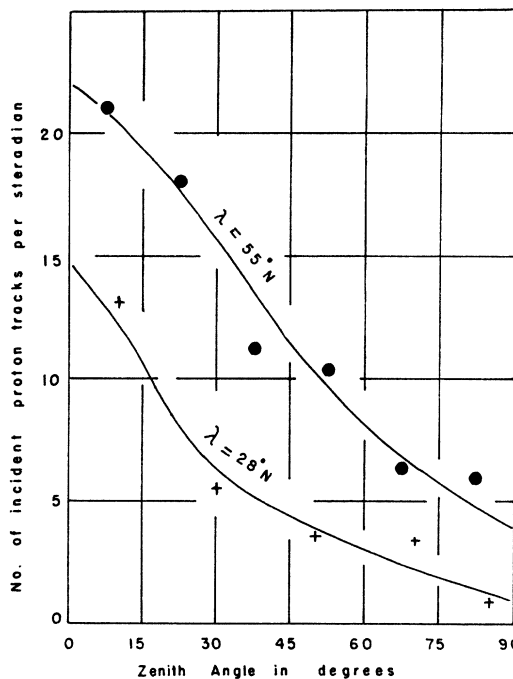


FIG. 7. Zenith angle dependence of all protons producing stars at 94,000 feet and $\lambda \approx 54^\circ$ and $\lambda \approx 28^\circ$.

stars by particles of type a per cc per day. Camerini, *et al.*¹⁶ have shown that the collision mean free paths, L_a , correspond very nearly to values equal to the average geometrical cross-sectional area of nuclei in the emulsion. Using this mean free path gives the values of the flux of particles initiating stars at $\lambda \approx 54^\circ$ and $\lambda \approx 28^\circ$ in Table V.

The flux of the total star-producing protons at 1.1-cm Hg pressure varies by a factor of 3.0 between $\lambda \approx 28^\circ$ and $\lambda \approx 54^\circ$, while the total neutrons which predominantly produce stars of 3 to 9 prongs vary by a factor of 5.2. The large change in the neutron flux is most likely due to the relatively efficient production of low energy neutrons by the great number of low energy primary protons, alpha-particles, and heavy nuclei at $\lambda \approx 54^\circ$ N.

The variation with altitude of the rate of production

TABLE V. Flux of particles producing stars.

1 Incident particles	2 Rate of production of stars of 3 or more prongs per cc per day at 1.1-cm Hg pressure-altitude		3 Emulsion interaction mean free path in grams/cm ² L_a	4 Integrated flux of particles per second per cm ² at 1.1-cm Hg pressure J_a		5 Latitude effect flux at $\lambda \approx 54^\circ$ N flux at $\lambda \approx 28^\circ$ N
	$\lambda \approx 54^\circ$ N	$\lambda \approx 28^\circ$ N		$\lambda \approx 54^\circ$ N	$\lambda \approx 28^\circ$ N	
Protons	873	287	100	0.259±0.02	0.085±0.01	3.04±0.4
Neutrons	1400	266	100	0.414±0.03	0.079±0.01	5.2±0.5
Alpha-particles	107	25	39	0.012±0.003	0.0028±0.007	4.3±0.9
Heavy nuclei $Z \geq 6$	7.2	2.1				~3.4
Total	2390	575		0.68	0.17	4.0

¹⁶ Camerini, Fowler, Lock, and Muirhead, *Phil. Mag.* 41, 413 (1950).

TABLE VI. Altitude variation of flux of particles producing stars.

Pressure-altitude (cm Hg)	Particles producing stars									
	Protons		Integrated flux of star producing particles per second per cm ²				Neutrons		Alpha-particles	
	Rate of production of stars with more than 2 prongs per cc per day N_a		J_a		J_a		J_a		N_a	
	$\lambda \approx 54^\circ$	$\lambda \approx 28^\circ$	$\lambda \approx 54^\circ$	$\lambda \approx 28^\circ$	$\lambda \approx 54^\circ$	$\lambda \approx 28^\circ$	$\lambda \approx 54^\circ$	$\lambda \approx 28^\circ$	$\lambda \approx 54^\circ$	$\lambda \approx 28^\circ$
1.1	873	287	0.26	0.085	1400	266	0.41	0.079	107	25
3.5	446	96	0.132	0.029	1660	275	0.49	0.081	54	12
50.0	2.46		0.00070		23.14		0.0068			

of stars by protons, neutrons, and alpha-particles for 3 elevations is given in Table VI at $\lambda \approx 54^\circ$. The rate of production of stars by protons decreases rapidly from 1.1 to 50 cm Hg, while the rate of neutron produced stars reaches a definite maximum at about 3.5 cm Hg. Considerably fewer data are available for the higher energy neutrons producing stars of more than 16 prongs; however, within experimental error, they seem to vary in a manner similar to the total neutron flux which primarily produces stars up to 9 prongs.

(D) Zenith Angle Distribution of Protons Producing Stars

The zenith angle distribution was given previously¹⁷ for higher energy protons which produced at least two minimum ionization tracks in a nuclear interaction. In this case the incident energy was sufficiently higher than the magnetic cut-off, so that the protons entered the earth's atmosphere, isotropically distributed in the upper hemisphere. The observed distribution at 1.1-cm Hg pressure showed comparable numbers of incident protons for all zenith angles up to about 70° , and then the number decreased rapidly for larger angles. This distribution is in good agreement with that to be expected for high energy protons absorbed with a cross section slightly larger than the nuclear area.

The zenith angle distribution has now been determined for all protons, including those of lower energies, which produce stars. Plates from four different balloon flights at $\lambda \approx 54^\circ$ and from one at $\lambda \approx 28^\circ$ were employed. The zenith angles were measured for all incident protons and were grouped according to the number of tracks per unit solid angle at the zenith angle, θ . These data are given in Fig. 7 for the measurements at $\lambda \approx 54^\circ$ and $\lambda \approx 28^\circ$. The zenith angle distribution curve for the total number of protons is quite different from that for only those of very high energy. This is to be expected, since the cross section for energy loss due to ionization of low energy protons becomes comparable to that due to nuclear collisions, which would tend to make the curve steeper. It is to be noted that the curve at $\lambda \approx 54^\circ$, Fig. 7 falls to half-intensity at an angle of $\theta = 47^\circ$, while the corresponding curve at $\lambda \approx 28^\circ$ reaches half-intensity at $\theta = 26^\circ$. This is probably owing to the larger influence

of the azimuthal variation of the magnetic cutoff of the earth¹⁵ at $\lambda \approx 28^\circ$ and the greater fraction of the secondary protons produced by primary alpha particles and heavy nuclei at $\lambda \approx 28^\circ$ than at $\lambda \approx 54^\circ$.

IV. CONCLUSIONS

The altitude dependence of nuclear disintegrations extending from 1.1 cm Hg down to sea level and the flux of star producing radiation give a considerable amount of information concerning the nature of the nuclear interactions of primary cosmic-ray particles and the energies of the particles initiating stars in the atmosphere.

From the data presented in this paper the following conclusions can be drawn.

(1) Neutrons at $\lambda \approx 54^\circ$ account for 56, 76, and 91 percent of the total stars at, respectively, 1.1-, 3.5-, and 50-cm Hg pressure. The flux of neutrons producing stars of more than two prongs reaches a broad maximum near 3.5 cm Hg (Fig. 8). The calculation of Bethe, Korff, and Placzek¹⁸ showed that the slowing down process for fast neutrons would result in a maximum in the intensity of slow neutrons at a distance of about 1 meter of water equivalent from the top of the atmosphere. Yuan¹⁹ has found a maximum in the slow neutron intensity at about 8 to 9 cm Hg, which is in good agreement with both the calculations of these authors¹⁸ and the maximum in the intensity of star producing neutrons near 3.5 cm Hg as given in this paper.

It remains as an interesting problem to determine the intensity of star-producing neutrons at altitudes greater than 1.1 cm Hg, where it is only 15 percent lower than at the maximum. At still higher altitudes it should then decrease very rapidly, since the neutrons must be secondary in origin.

(2) At 1.1-cm Hg pressure ($\lambda \approx 54^\circ N$) only about 23 percent of the stars with more than 16 prongs are produced by high energy neutrons; the remaining 69 percent and 8 percent are produced, respectively, by protons and α -particles. The corresponding figures for neutrons are 45 percent at 3.5 cm Hg and 50 percent at 50 cm Hg. Considering that stars of more than 16 prongs are only moderately sensitive to latitude (Fig. 6),

¹⁷ J. J. Lord and M. Schein, Phys. Rev. **77**, 25 (1950).

¹⁸ Bethe, Korff, and Placzek, Phys. Rev. **57**, 573 (1940).

¹⁹ L. C. L. Yuan, Phys. Rev. **77**, 728 (1950).

it follows that 43 percent of them must be produced by particles of energies in excess of that given by the magnetic cut-off of the earth¹⁵ at $\lambda \approx 28^\circ\text{N}$ (8 Bev for protons and 3.5 Bev per nucleon for α -particles and heavier nuclei). The variation with altitude of the flux of these high energy star-producing neutrons, Fig. 8, shows little change between 1.1 and 3.5 cm of Hg, which demonstrates that a large fraction of them are of secondary origin.

(3) Measurements of the rate of production of stars by ionizing incident particles shows that at 1.1-, 3.5-, and 50-cm Hg pressure protons produce, respectively, 69, 55, and 50 percent of the total stars of more than 16 prongs. This, in contrast to the high energy star producing neutrons, shows (Fig. 4) that the number of high energy protons initiating stars decreases rapidly with altitude at the highest elevations (1.1 cm Hg). This shows that a part of these stars must be produced by primaries of even stronger absorption close to the top of the atmosphere.

The variation with altitude of the flux of protons producing all stars of more than 2 prongs is given in Fig. 8 and is in good agreement with an absorption mean free path of 145 g/cm².

(4) The rate of production of stars by alpha-particles at 1.1-cm Hg pressure amounts to approximately 5 percent of the total star production at both $\lambda \approx 54^\circ$ and $\lambda \approx 28^\circ$. This figure, which is low compared to the known primary flux,²⁰ is apparently due to the rapid absorption of the α -particles incident isotropically in the upper hemisphere at the top of the atmosphere.

(5) The total rate of production of stars with two or more prongs at $\lambda \approx 54^\circ$ and 1.1-cm Hg pressure is 3.85 times the corresponding value at $\lambda \approx 28^\circ$. Most of this increase is due to the large rate of production of small stars by neutrons, which varies by a factor of 5.2 between the above-mentioned latitudes and which is the largest latitude effect which has been observed for any component of the cosmic radiation so far. Taking into account the magnetic cut-off for 54°N and 28°N this shows that 81 percent of the neutrons initiating stars

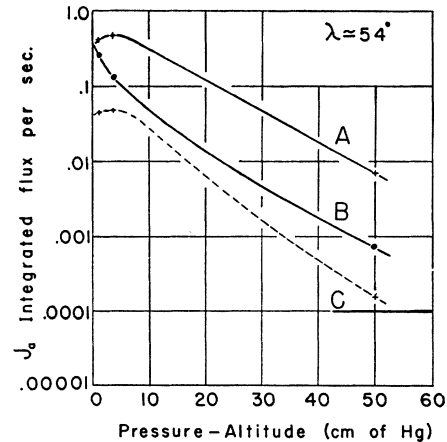


Fig. 8. Integrated flux of star-producing particles as a function of pressure-altitude. Curve *A*—total flux of neutrons producing stars of more than 2 prongs; curve *B*—total flux of protons producing stars of more than 2 prongs; curve *C*—flux of neutrons producing stars of more than 16 prongs.

are produced by primary particles of energies between 1 and 8 Bev for protons and 0.35 to 3.5 Bev per nucleon for α -particles and heavier nuclei. Since within these energy limits meson production is small, most of the primary energy in collisions with air nuclei goes into the production of secondary nucleons.

The variation of the star-producing proton flux between the above latitudes was 3.0 (Table V), which within statistical error is in agreement with the measurements of other authors.²¹ This shows that 67 percent of the proton-initiated stars at $\lambda \approx 54^\circ$ arise from primary particles in the above-mentioned energy intervals imposed by the magnetic cutoff of the magnetic field of the earth.

It is a pleasure to acknowledge the advice and encouragement of Professor Marcel Schein who suggested this work. I should also like to thank Professor Metcalf, director of the Athletic Department, for his competent assistance in making the athletic field available for balloon flights.

²⁰ H. L. Bradt and B. Peters, Phys. Rev. **77**, 54 (1950).

²¹ Salant, Hornbostel, Fisk, and Smith, Phys. Rev. **79**, 184 (1950); Winckler, Stix, Dwight, and Sabin, Phys. Rev. **79**, 656 (1950).